JIRRS
Journal International Review of Research Studies

**Received:** 13/06/2026 - **Accepted:** 07/11/2026
**Vol**: 1.11
**DOI**: 10.66104/dr86mq28
**Pages:** 1-34

# Vanadium Distribution and Competing Slag Associations in Reductive Smelting of Spent NiMoV Catalysts: Oxygen Potential, Aluminosilicate Interactions, and Metal Recovery Constraints—A Critical Review

**Antonio Clareti Pereira, Ph.D.**
Department of Graduate Program in Materials Engineering
Federal University of Ouro Preto (UFOP)
Ouro Preto, Minas Gerais, Brazil
**E-mail:** claretipereira@gmail.com
**ORCID:** https://orcid.org/0000-0001-8115-4279

## Abstract

Spent Ni–Mo–V hydroprocessing catalysts are alumina-rich secondary resources whose reduction smelting produces valuable metal alloys and complex oxide slags. This critical narrative review addresses where vanadium resides when it is not recovered in the bulk alloy. It contrasts direct experimental evidence with thermodynamic and mechanistic analogs, explicitly separating vanadium dissolved in liquid slag, retained in crystalline oxides, entrained as metallic droplets, and transferred to dust or deposits. Under different operating configurations, reported V recoveries range from 25.1% in reduction–sulfurization smelting to 89.7% in reduction smelting of mixed catalyst/ore feeds; an independent optimized kilogram-scale catalyst-smelting study reported 97.9%. These process recoveries are not equilibrium partition coefficients and cannot be transferred across feed and slag systems. We formalize phase-specific vanadium inventories, recovery, and mass-balance closure, and assess the coupled roles of oxygen potential, carbon and sulfur activities, aluminosilicate chemistry, crystallization, liquidus margin, and droplet settling. The review presents a diagnosis-first framework for distinguishing chemical retention from physical separation losses and identifies the experimental data needed for process optimization and scale-up.

**Keywords:** vanadium partitioning; spent hydroprocessing catalysts; reductive smelting; oxygen potential; spinel; slag engineering

## Highlights

1. • Vanadium distribution is governed jointly by oxygen potential, oxide phases, and alloy separation.
2. • Bulk slag assays cannot distinguish chemical retention from entrained alloy droplets.
3. • High-alumina slag chemistry and spinel formation constrain vanadium recovery.
4. • Phase-resolved balances offer a practical basis for diagnosing recovery losses.

JIRRS
Journal International Review of Research Studies

**Received:** 13/06/2026 - **Accepted:** 07/11/2026
**Vol**: 1.11
**DOI**: 10.66104/dr86mq28
**Pages:** 1-34

## Graphical Abstract

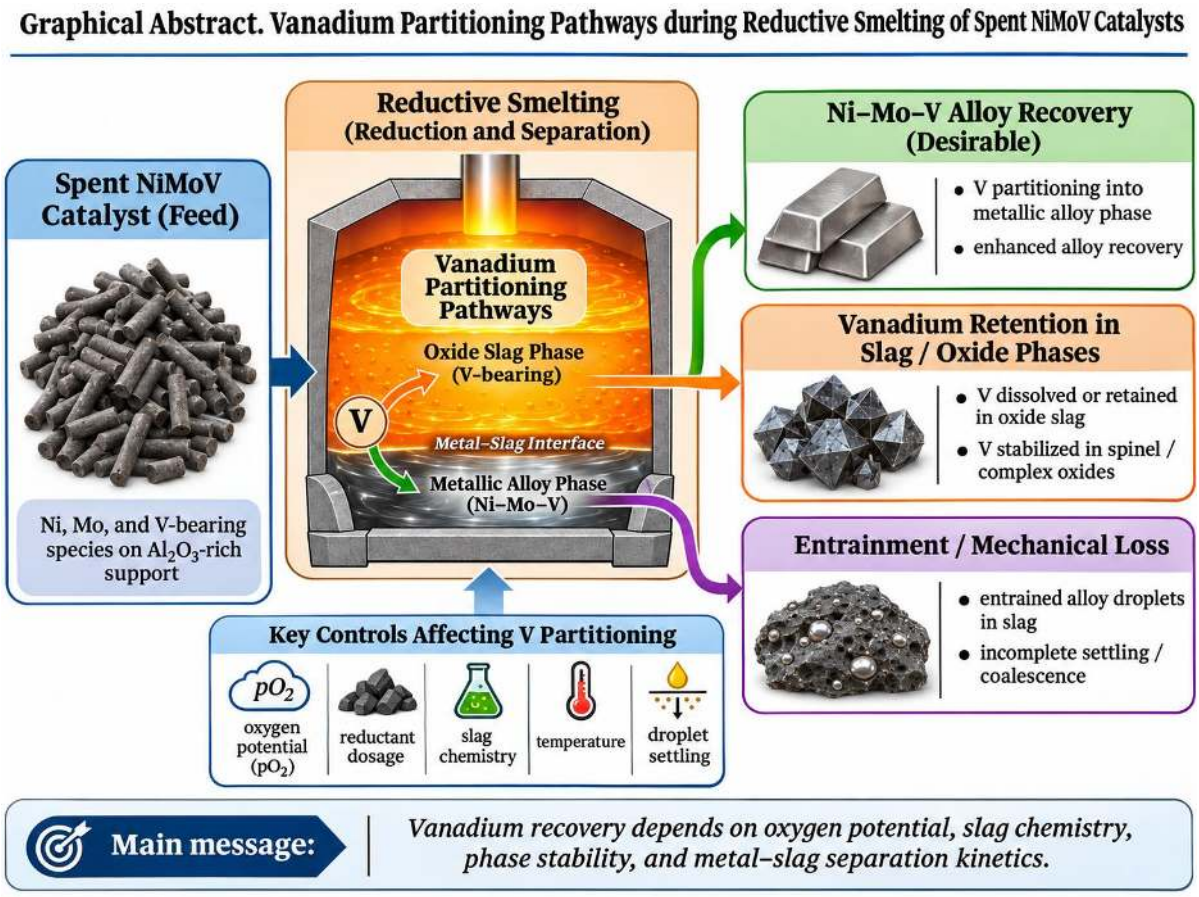


## 1. Introduction

Spent hydrotreating and hydroprocessing catalysts contain economically relevant Ni, Mo, and V on supports often rich in $Al_2O_3$, along with deposited sulfur, carbon, iron, and other process-derived constituents. Feed pretreatment and flux addition modify both the available metal inventory and the oxide-phase environment; the alumina support is therefore not inert gangue. Although recent reviews have addressed general catalyst pretreatment, metal recovery, and total resource utilization (Ying et al., 2025; Tian et al., 2026), this review focuses on a narrower question: the physical and chemical destination of vanadium during reductive smelting. This critical narrative review focuses on the evidence required to distinguish liquid-slag dissolution, V-bearing crystalline phases, entrained V-bearing alloy droplets, captured dust and deposits, and unresolved inventory. Previous reviews of spent-catalyst recycling, slag-property control, Fe–C–V metallurgy and metal-droplet coalescence

JIRRS
Journal International Review of Research Studies
**Received:** 13/06/2026 - **Accepted:** 07/11/2026
**Vol**: 1.11
**DOI**: 10.66104/dr86mq28
**Pages:** 1-34

(Pereira et al., 2026a–e) address related processing principles; the present work instead integrates those principles into a V-specific, phase-resolved destination and diagnostic framework, without presenting the earlier topics as independent novelty claims.

The contrast between direct studies illustrates the problem. Shi et al. (2023) reported 97.9% V recovery under an optimized 1500 °C kilogram-scale reduction-smelting configuration. In contrast, Wang et al. (2023) recovered only 25.1% V (despite 91.1% Ni and 92.9% Mo) during reduction–sulfurization smelting at 1450 °C in an $Al_2O_3$–FeO–$SiO_2$ slag, and approximately 89.7% V during a different reduction-smelting configuration at 1525 °C in an $Al_2O_3$–MgO–$SiO_2$ system. These are not controlled single-variable sulfur experiments: feed blend, fluxes, temperature, and process architecture also differ. Accordingly, high Ni/Mo recovery does not guarantee high V recovery, and low V collected in bulk alloy need not mean insufficient chemical reduction.

The objectives are to (i) define robust measures of vanadium deportment; (ii) examine oxidation-state and slag-composition controls; (iii) distinguish incorporation in metal from oxide retention; (iv) separate chemical from mechanical losses; and (v) identify experimental reporting needed for scale-up. Figure 1 summarizes the conceptual basis of the material pathways, while Figures 2–4 map oxygen-potential effects, slag modifiers, and diagnostic interventions. Tables 1–7 summarize the characterization, evidence hierarchy, mechanisms, diagnostic criteria, and phase-resolved accounting requirements required to attribute vanadium by phase.

JIRRS
Journal International Review of Research Studies

**Received:** 13/06/2026 - **Accepted:** 07/11/2026
**Vol**: 1.11
**DOI**: 10.66104/dr86mq28
**Pages:** 1-34

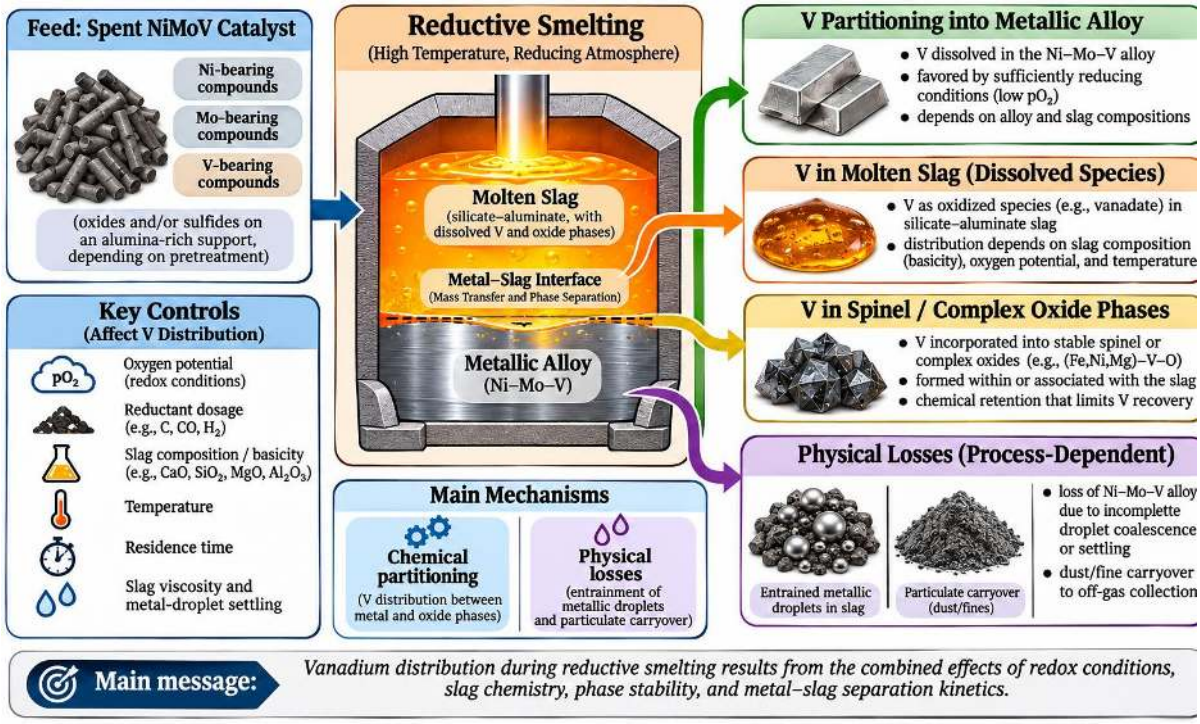


**Figure 1.** Conceptual distribution of vanadium between recoverable alloy, oxide melt, crystalline slag phases, entrained metal, and dust. Original synthesis; all terms must be measured or bounded experimentally.
Editorial verification required before publication: the author must confirm graphical provenance, ownership, and any adaptation permissions; this revision asserts no license clearance.

## 2. Review Methodology and Vanadium Partitioning Evidence

This is a critical narrative review, not a systematic review. The original bibliography comprises 140 reference entries; the targeted revision checked additional primary and review sources through publisher article pages and PubMed records up  Augus 2026, verifying Wang et al. (2023), Ying et al. (2025), and Tian et al. (2026). Representative verification queries combined “spent hydrogenation catalyst”, “vanadium”, “reduction sulfurization”, “slag”, “metal recovery”, “spinel,”, and “phase distribution”. No exhaustive, reproducible database search, screening flowchart, or formal risk-of-bias assessment was performed; results should not be described as comprehensive or systematically screened. The evidence classes are (A) direct spent-catalyst smelting, (B) controlled metal–slag or phase-equilibrium measurements, and (C) mechanistic analogs from ironmaking and V slags. The revision does not assume that analogs quantitatively predict Ni–Mo–V smelting results.

JIRRS
Journal International Review of Research Studies

**Received:** 13/06/2026 - **Accepted:** 07/11/2026
**Vol**: 1.11
**DOI**: 10.66104/dr86mq28
**Pages:** 1-34

We evaluate evidence strength against actual feed, alloy solvent, sulfur and carbon activity, oxygen potential, flux composition, temperature, phase separation, thermal history, and elemental accounting. Studies reporting only recovery or bulk-slag assays cannot independently establish phase equilibrium. We checked the quantitative values cited in the revised discussion of Wang et al. (2023) against the publisher abstract and article; independently audit other historic source-level figures and bibliographic metadata against original publications before submission. Tables and equations below are a methodological synthesis, not newly generated experimental data.

### 2.1 Operational definitions

On an elemental mass basis, $R_{V,alloy} = m_{V,recovered\ bulk\ alloy}/m_{V,feed}$ (1). For homogeneous coexisting liquid phases under defined conditions, $L_V^{\{slag/metal\}} = w_{V,liquid\ slag}/w_{V,liquid\ metal}$ (2), where w is the elemental V mass fraction. This is a concentration ratio, not a thermodynamic equilibrium constant. A slag assay combining oxide liquid, crystals, and entrained alloy cannot replace the liquid-slag numerator. A complete output inventory must separately identify recovered metal, dissolved oxidic V, V-bearing crystalline oxides, uncollected metal droplets, dust/off-gas capture, wall deposits, and unresolved material.

The phase-resolved elemental accounting basis is $m_{V,F} = m_{V,A} + m_{V,S,diss} + m_{V,S,cryst} + m_{V,entr} + m_{V,dust} + m_{V,wall} + m_{V,other}$ (3), with F = feed and A = physically collected alloy. The measured-output closure statistic is $C_V$ (%) = 100 × [Σ $m_{V,measured\ outputs}$]/$m_{V,F}$ (4); an unresolved difference must be disclosed instead of forced into a measured phase. Define $f_{V,chem} = [m_{V,S,diss}+m_{V,S,cryst}]/m_{V,F}$, $f_{V,entr} = m_{V,entr}/m_{V,F}$, and $f_{V,dust} = m_{V,dust}/m_{V,F}$. With wall and other losses included consistently, $R_{V,alloy}+f_{V,chem}+f_{V,entr}+f_{V,dust}+f_{V,wall}+f_{V,other} = 1$ subject to reconciled uncertainty (5). These are accounting identities, not empirical recovery correlations.

Particular care is needed when reporting a low V concentration in slag: the result may reflect effective metal reduction, dilution by flux addition, partition into unexamined solid phases, or non-representative sampling. A credible comparison across studies therefore requires both the composition and mass of each stream, measured oxidation environment, phase identification, and analytical uncertainty.

JIRRS
Journal International Review of Research Studies
**Received:** 13/06/2026 - **Accepted:** 07/11/2026
**Vol**: 1.11
**DOI**: 10.66104/dr86mq28
**Pages:** 1-34

For any identified phase k, phase-specific deportment is $D_{V,k} = m(k)w_{V,k}/m_{V,F}$ (6). Alloy yield $Y_A = m(A)/m(\text{dry feed})$, and $m_{V,A} = Y_A w_{V,A} m(\text{dry feed})$ (7). For comparison across feed grades, report $I_V = m_{V,A}/m(\text{dry spent catalyst})$, preferably in kg V/t dry catalyst, alongside kg alloy/t dry catalyst. For a slag, $m_{V,slag} = m(slag)w_{V,slag}$; lower slag wt% V after flux addition can reflect dilution and must never by itself be interpreted as higher recovery. Phase fractions, representative sampling, and propagated assay/mass uncertainty are essential.

## 3. Vanadium-Bearing Species in Spent Catalyst Feedstocks

Vanadium can occur in service-aged catalysts as sulfide-related species, oxidized surface compounds, or complex associations with alumina and deposited metals. The feed composition evolves during washing, decoking, and oxidative treatment, so the phase assemblage entering the smelter need not match that of the spent catalyst as received. Alumina from the original support typically contributes significantly to the final slag, while iron, calcium, silicon, sodium, magnesium, and other additions alter its structure and liquidus.

Direct quantitative identification of V valence in heterogeneous spent catalyst feed requires a combined characterization protocol, not a single technique. Bulk X-ray fluorescence or inductively coupled plasma analysis establishes elemental inventories; X-ray diffraction distinguishes detectable crystalline phases; electron microscopy can identify V-rich domains and intergrowths; and properly interpreted X-ray photoelectron spectroscopy may constrain surface oxidation states. Do not extrapolate the latter to bulk composition without complementary measurements.

Feed characterization should report representative sampling, moisture and carbon loss, sulfur oxidation products, and the elemental inventory before and after pretreatment. If these variables are omitted, apparent differences in smelting recovery may instead arise from changing mass bases and feed heterogeneity.

Table 1 organizes the following synthesis to compare mechanisms and evidentiary requirements across the available studies.

**Table 1.** Feed characterization variables and their implications for vanadium deportment.

| Feed variable | Analytical approach | Implication for interpretation |
|---|---|---|

JIRRS
Journal International Review of Research Studies
**Received:** 13/06/2026 - **Accepted:** 07/11/2026
**Vol**: 1.11
**DOI**: 10.66104/dr86mq28
**Pages:** 1-34

| Feed variable | Analytical approach | Implication for interpretation |
|---|---|---|
| Bulk Ni, Mo, V and support oxides | Representative sampling; XRF or ICP-based assay | Sets the elemental input inventory and expected slag burden |
| Carbon and sulfur deposits | Carbon/sulfur analyses before and after pretreatment | Changes reductant/oxygen demand and apparent recovery mass basis |
| V-bearing surface and crystalline species | XRD, microscopy, and cautiously interpreted XPS | Surface speciation alone does not establish bulk V oxidation state |
| Particle and support heterogeneity | Particle-size fractions; cross-sectional SEM–EDS | Segregation may bias feed sampling and phase inventories |

*Note.* Critical synthesis of the cited literature and methodological recommendations; no new experimental measurements are reported.

Table 1 shows why feed characterization should precede any comparison of reductive-smelting recoveries. The proposed analyses are diagnostic requirements, not a dataset measured for the present review.

## 4. Vanadium Metal–Slag Equilibria

Vanadium partitioning at smelting temperature is governed by equality of chemical potential across coexisting phases. The resulting V content of metal and slag depends on oxygen potential, melt structure, temperature, alloy composition, and activity coefficients. Wright and Davidson (2021) measured vanadium distribution between carbon-saturated iron and an $Al_2O_3$–CaO–MgO–$SiO_2$–$TiO_2$ slag under controlled atmosphere at 1400–1500 °C, providing a useful equilibrium reference. Their results cannot be transferred numerically to Ni–Mo–V alloys because the metal solvent, phase saturation, and slag environment differ.

For direct spent-catalyst smelting, Shi et al. (2023) reported 98.3% Ni, 95.3% Mo, and 97.9% V recoveries in a kilogram-scale test at 1500 °C with a specified flux/reductant recipe. The case strongly supports alloy capture as a viable destination for V. However, a single optimized condition does not determine universal metal–slag equilibrium constants, and the reported recovery encompasses chemical and physical separation phenomena. Direct phase equilibria must be distinguished from reactor-scale yield.

In the direct mixed-waste study of Wang et al. (2023) [class A], reduction–sulfurization smelting at 1450 °C for 2 h with $Al_2O_3$–FeO–$SiO_2$ slag yielded 91.1% Ni, 92.9% Mo, and 25.1% V recovery. Characterization identified V associated with ferro- or aluminosilicate environments, consistent with selective V retention under those tested conditions. A separate reduction-smelting configuration at 1525 °C, with a different feed/slag

JIRRS
Journal International Review of Research Studies
**Received:** 13/06/2026 - **Accepted:** 07/11/2026
**Vol**: 1.11
**DOI**: 10.66104/dr86mq28
**Pages:** 1-34

arrangement based on $Al_2O_3$–MgO–$SiO_2$, yielded approximately 96.8% Ni, 96.7% Mo, and 89.7% V. The comparison demonstrates process sensitivity but does not isolate a unique sulfur effect because multiple variables changed together. Wang et al. (2023) and Shi et al. (2023) should therefore be compared as distinct process demonstrations, not as interchangeable V partition-equilibrium datasets.

A rigorous equilibrium study should state reference oxygen potential or $CO/CO_2$ conditions, temperature, approach-to-equilibrium time, saturation constraints, both bulk and liquid-phase compositions, carbon activity, and how metal and slag samples were quenched. Compare thermodynamic calculations with phase-specific measurements rather than using them as a replacement.

Table 2 organizes the following synthesis to compare mechanisms and evidentiary requirements across the available studies.

**Table 2.** Evidence hierarchy for interpreting vanadium metal–slag distribution.

| Evidence setting | What can be established | Transferability limitation |
|---|---|---|
| Direct spent-catalyst smelting (Shi et al., 2023) | Feasibility and reactor-scale elemental recovery under tested conditions | Combines reduction, phase chemistry, and physical separation |
| Controlled Fe–slag equilibration (Wright & Davidson, 2021) | Equilibrium partitioning within the measured solvent/slag domain | Carbon-saturated Fe is not a Ni–Mo–V alloy |
| V-rich FeO–$SiO_2$ slag phase studies (Lindvall et al., 2017) | Phase relations and composition-sensitive V association | Slag and alloy compositions differ from catalyst-derived systems |
| Thermodynamic model projections | Hypotheses for phase stability and sensitivity | Require calibrated databases and measured validation |

*Note.* Critical synthesis of the cited literature and methodological recommendations; no new experimental measurements are reported.

The comparison in Table 2 distinguishes experimentally observed recovery from equilibrium measurements and mechanistic analogies. Numerical distribution ratios should not be transferred across these systems without validation.

## 5. Oxidation State and Oxygen Potential Dependence

Vanadium exhibits multiple oxidation states in metallurgical oxide systems. Depending on $pO_2$ and temperature, higher-valence oxides can be stabilized under more oxidizing conditions while lower-valence oxides and, under sufficiently reducing conditions,

JIRRS
Journal International Review of Research Studies
**Received:** 13/06/2026 - **Accepted:** 07/11/2026
**Vol**: 1.11
**DOI**: 10.66104/dr86mq28
**Pages:** 1-34

metal-bearing phases become favorable. This relationship is not an isolated redox ladder: the stability of V-containing species depends on activities in the multicomponent slag and on V solubility in the receiving alloy.

Reductant mass is an operating input, not a measurement of oxygen potential. Where available, report $\log_{10}(pO_2/\text{reference pressure})$, the reference state and operating temperature, gas $CO/CO_2$ ratio, carbon activity, oxide activities, gas flow, and the measurement or equilibrium-inference method. Sulfur is an independent process variable: sulfide/sulfate chemistry, pyrite addition, sulfur volatilization, and possible matte formation influence V transfer and phase identification. In Wang et al. (2023), V-bearing aluminosilicate associations and changing FeO-rich slag chemistry accompany reduction–sulfurization; neither a universal sulfur penalty nor a causal effect of sulfur alone is established.

A common error is to interpret an increase in reductant addition as proof that all residual V exists as unreduced oxide. Carbon can change oxygen potential and influence other elements, whereas viscosity, temperature, and interfacial dynamics determine whether the reduced metal is actually recovered. Consequently, the qualitative pathways in Figure 2 do not define universal transition boundaries; quantitative stability diagrams require a selected reference state and a thermodynamic database appropriate to the investigated slag.

JIRRS
Journal International Review of Research Studies

**Received:** 13/06/2026 - **Accepted:** 07/11/2026
**Vol**: 1.11
**DOI**: 10.66104/dr86mq28
**Pages:** 1-34

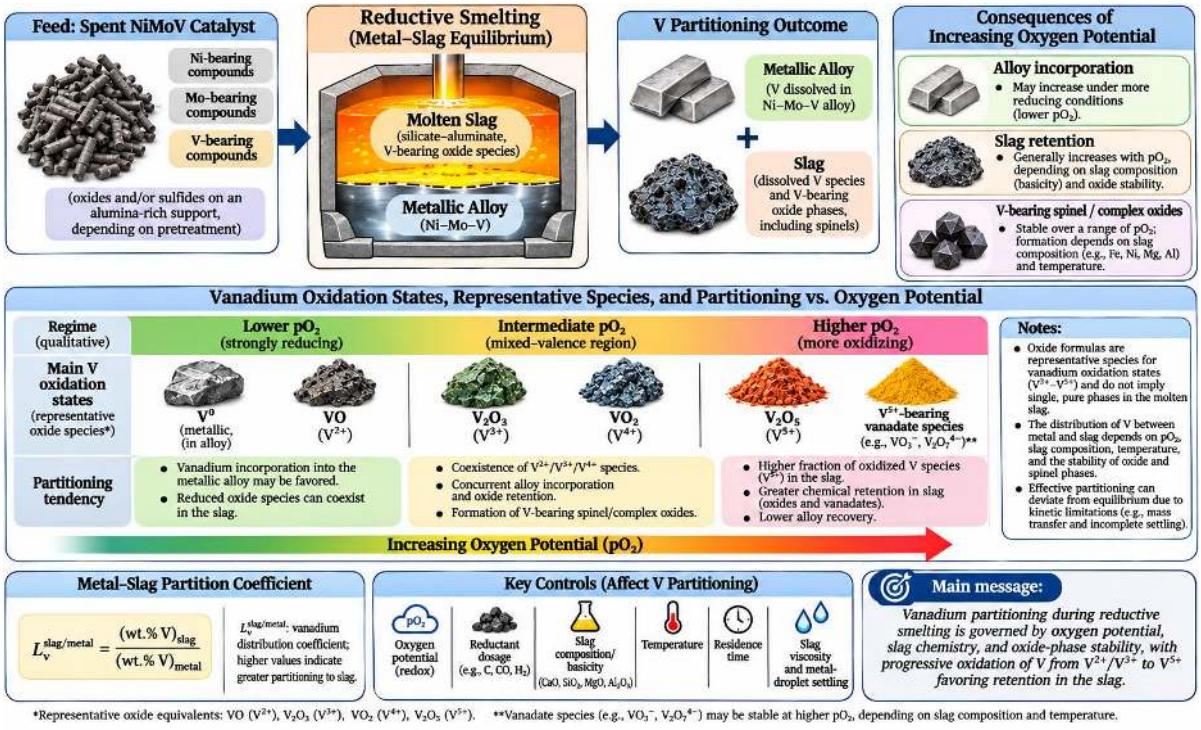


**Figure 2.** Conceptual changes in vanadium speciation and phase preference with oxygen potential.
Original interpretation; no numerical phase boundaries or equilibrium lines are implied.
Editorial verification required before publication: author must confirm graphical provenance, ownership, and any adaptation permissions; this revision asserts no license clearance.

A recommended experimental design varies reductant level and atmosphere independently where possible, while measuring dissolved V in slag, V associated with solid phases, and alloy composition. This separates changes in oxidation state from changes in recovery due to settling. Document quenching conditions and sample exposure after smelting to prevent reoxidation from confounding oxidation-state assays.

Table 3 organizes the following synthesis to compare mechanisms and evidentiary requirements across the available studies.

**Table 3.** Oxygen-potential controls and diagnostic observations for vanadium.

| Variable or observation | Expected interpretive role | Essential qualification |
|---|---|---|
| Gas atmosphere/oxygen potential | Controls relative stability of V-bearing oxidation states | Report temperature and reference conditions |
| Carbon addition and carbon activity | Changes reducing capacity and coupled oxide reactions | Reductant dose is not a direct $pO_2$ measurement |
| Alloy V assay and mass | Quantifies collected elemental V | Does not independently identify oxide/metal equilibrium |

JIRRS
Journal International Review of Research Studies
**Received:** 13/06/2026 - **Accepted:** 07/11/2026
**Vol**: 1.11
**DOI**: 10.66104/dr86mq28
**Pages:** 1-34

| Variable or observation | Expected interpretive role | Essential qualification |
|---|---|---|
| Dissolved and crystalline slag V | Distinguishes different oxidic retention pathways | Quenching can generate secondary phases |
| Entrained alloy droplets | Identifies reduced V not collected in bulk alloy | Requires microscopy and phase separation |

*Note.* Critical synthesis of the cited literature and methodological recommendations; no new experimental measurements are reported.

As summarized in Table 3, a measured improvement in recovery alone is insufficient to infer a redox transition. Combined gas, phase, and mass observations are needed.

## 6. Vanadium Association with Alumina and Silicate Phases

The alumina support is not an inert mass sink. Upon fusion, $Al_2O_3$ participates in the structure and liquidus of calcium–aluminosilicate slags. Vanadium can remain dissolved in the oxide melt or become enriched in crystalline phases, including spinel-type structures under suitable composition and redox conditions. Crystallization studies of vanadium-bearing steelmaking slags, such as Diao et al. (2016, 2018, 2024), substantiate the importance of growth mechanisms and competition among solid phases. These studies supply mechanistic analogies, not direct measurements of spent NiMoV smelting outcomes.

Lindvall, Berg, and Sichen (2017) investigated the effects of $Al_2O_3$, CaO, and $SiO_2$ on FeO–$SiO_2$ slags containing vanadium, whereas Lindvall, Tikka, Berg, Ye, and Sichen (2017) examined vanadium transfer from a Fe–V–P melt and the associated slag phase relations. Although these studies inform oxide-network effects and V-bearing phase stability, their Fe-rich metallic solvent and specific slag compositions do not match a Ni–Mo–V catalyst-smelting system. Direct measurements in high-alumina, Ni-bearing environments remain necessary.

An oxide spinel identified after cooling may have crystallized during quenching rather than being present as a high-temperature equilibrium solid. Report cooling rates, quench geometry, thermodynamic predictions of high-temperature phase fractions, and sensitivity to thermal history. Where XPS is used, surface valence must not be extrapolated to bulk vanadium without XANES/XAS or another complementary phase-sensitive bulk measurement. Oxidation state and process destination are non-equivalent descriptors.

Evidence for spinel retention should be based on spatially resolved elemental analysis and phase identification, not merely on an elevated bulk slag V concentration. Where quantitative microscopy is used, reporting phase fractions, grain-size distribution, and the V

JIRRS
Journal International Review of Research Studies
**Received:** 13/06/2026 - **Accepted:** 07/11/2026
**Vol**: 1.11
**DOI**: 10.66104/dr86mq28
**Pages:** 1-34

concentration within each phase will permit estimation of phase-specific V inventories. Solid phases formed during cooling must be distinguished from phases that were stable at the smelting temperature.

**7. Effects of CaO, $SiO_2$, MgO, and Slag Modifiers**

Slag modifiers have coupled thermodynamic and transport effects. CaO changes basicity, phase stability, and the extent to which the aluminosilicate network depolymerizes; $SiO_2$ and $Al_2O_3$ contribute to network formation and phase equilibria; MgO can affect both melt properties and spinel stability. Additives such as $Na_2O$ or $B_2O_3$ may lower melting temperature in selected compositions, but can introduce volatility, refractory, or downstream management constraints. Simple indices such as $CaO/SiO_2$ cannot capture all of these interacting variables.

In the smelting study of Shi et al. (2023), flux design was used to obtain a fluid high-alumina slag and improve alloy recovery. This is important because alloy formation without effective phase disengagement can still yield poor collection. Conversely, a slag formulation that lowers viscosity may increase V solubility or alter the solid phase assemblage. Therefore, lower viscosity does not automatically mean lower chemical retention.

A useful operating descriptor is liquidus margin $\Delta T_L = T_{process} - T_{liquidus}$ (8), reported together with liquid fraction, crystalline solids fraction, crystal morphology, slag viscosity and refractory compatibility. The optimum for fluidity need not be the optimum for chemical V retention. Fluxing with $Na_2O/B_2O_3$ may enhance settling in selected slags but can also alter V activity, volatilization and refractory attack. An overall basicity ratio alone cannot describe this multidimensional response.

Figure 3 synthesizes the principal competing effects. The preferred design should minimize total unrecovered V while satisfying a liquidus margin, acceptable viscosity, refractoriness, alloy settling behavior, and an environmental specification for the solidified slag. Multivariate designs and validated thermodynamic calculations are preferable to single-factor generalizations.

JIRRS
Journal International Review of Research Studies

**Received:** 13/06/2026 - **Accepted:** 07/11/2026
**Vol**: 1.11
**DOI**: 10.66104/dr86mq28
**Pages:** 1-34

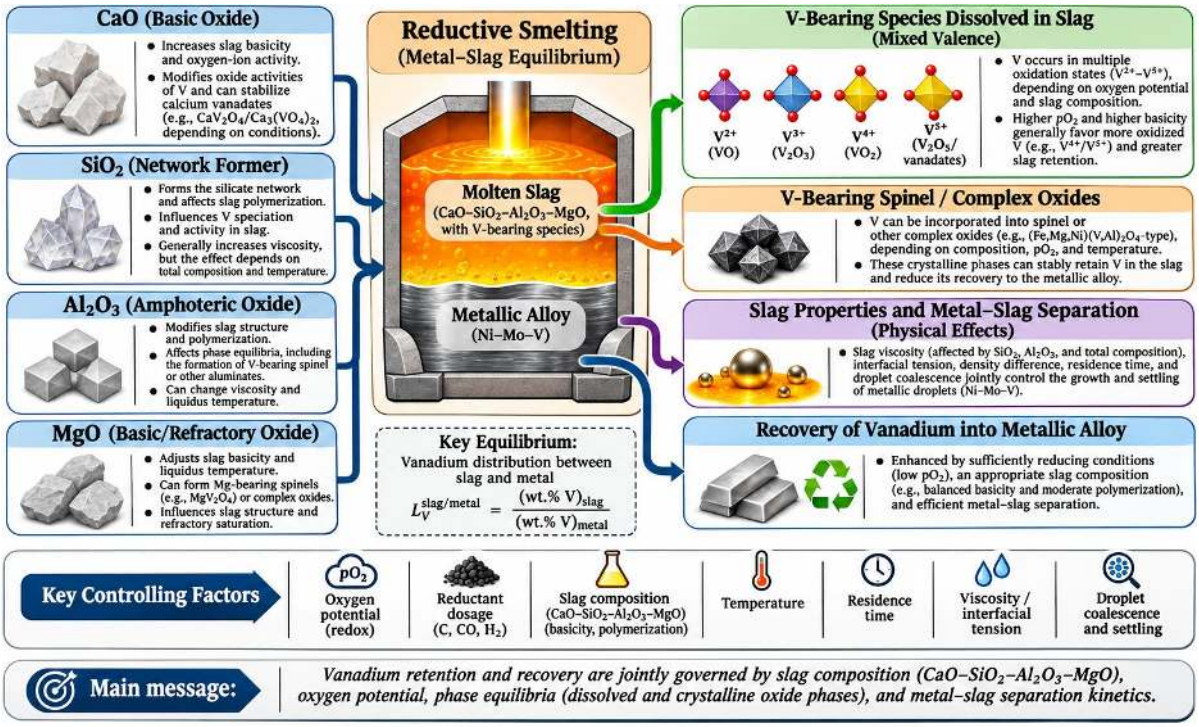


**Figure 3.** Qualitative network of CaO, $SiO_2$, $Al_2O_3$, and MgO effects on oxide activities, slag phases, and vanadium recovery. Adapted conceptually from the mechanisms discussed in the cited literature; original schematic.
Editorial verification required before publication: author must confirm graphical provenance, ownership, and any adaptation permissions; this revision asserts no license clearance.

The following synthesis is organized in Table 4 to compare mechanisms and evidentiary requirements across the available studies.

**Table 4.** Coupled functions and trade-offs of slag-forming components.

| Component | Relevant functions | Design trade-off/verification |
|---|---|---|
| CaO | Modifies basicity, oxide activities, and liquidus relations | Check predicted phases, viscosity, and refractory compatibility |
| $SiO_2$ | Contributes to network structure and silicate phase stability | Changes viscosity and V-bearing phase associations |
| $Al_2O_3$ | Major support-derived slag constituent; alters liquidus | High-alumina slags may demand composition-specific fluxing |
| MgO | Affects melt chemistry and Mg-bearing spinel stability | Confirm saturation and crystalline retention |
| $Na_2O$ / $B_2O_3$ additions | Potential fluxing in selected slag compositions | Evaluate volatility, refractory attack, and residue management |

*Note.* Critical synthesis of the cited literature and methodological recommendations; no new experimental measurements are reported.

Table 4 emphasizes that no single basicity index captures simultaneous changes in solubility, crystalline phases, viscosity, and metal-droplet separation.

JIRRS
Journal International Review of Research Studies
**Received:** 13/06/2026 - **Accepted:** 07/11/2026
**Vol**: 1.11
**DOI**: 10.66104/dr86mq28
**Pages:** 1-34

## 8. Vanadium Incorporation into Ni–Mo–V Alloys

The metallic product is a multicomponent solvent rather than a pure V phase. Nickel and iron can appear early during reduction and provide nuclei or metal droplets into which subsequently reduced Mo and V are incorporated. Shi et al. (2023) observed nickel/iron-rich matrix regions and molybdenum/vanadium-rich regions in the recovered alloy. Such microstructural partitioning affects the interpretation of bulk metal assays and the alloy's suitability for downstream refining.

The kinetic sequence of metal nucleation and growth is relevant only insofar as it affects V destination. For this review, the main distinction is between dissolved/alloyed V in recoverable bulk metal and V in dispersed metal droplets that are physically trapped within slag. Both may have identical or similar oxidation states but very different process remedies. Microprobe analysis, controlled remelting, and imaging of quenched slag can help separate the two.

The subsequent conversion of NiMoV alloy to separated metal products is a distinct processing stage. Shi et al. (2024) investigated oxidation leaching of an enriched alloy, confirming the relevance of a combined pyrometallurgical–hydrometallurgical processing concept. However, downstream leaching performance should not be conflated with the earlier metal–slag partition coefficient.

## 9. Chemical Retention and Mechanical Losses

Vanadium associated with an oxidic slag phase is a chemical or phase-equilibrium loss, whereas V-bearing metal droplets entrained in slag are a mechanical loss. In practice, a single bulk slag assay measures the sum. High viscosity, small droplets, unfavorable wetting, incomplete coalescence, turbulence, and insufficient residence time can inhibit metal collection. Settling behavior also depends on droplet density, size distribution, interfacial tension, and the presence of solid particles in slag.

A process diagnostic should divide slag vanadium into at least the following operational fractions: V in isolated metal inclusions, V in identifiable V-rich crystals, and V dispersed in the remaining oxide phase. Dust and deposits on reactor walls should be sampled

JIRRS
Journal International Review of Research Studies
**Received:** 13/06/2026 - **Accepted:** 07/11/2026
**Vol**: 1.11
**DOI**: 10.66104/dr86mq28
**Pages:** 1-34

where materiality warrants. Each fraction must be multiplied by its actual mass or estimated inventory; concentration percentages alone cannot close an elemental balance.

Poor recovery attributed solely to oxygen potential can lead to excessive carbon dosage when physical separation is the dominant issue. Conversely, reducing viscosity without adjusting oxide chemistry may not resolve V retained in stable crystals. The diagnosis must therefore precede the process correction.

For small, isolated spherical droplets settling in a Newtonian fully liquid slag under creeping-flow conditions, the scaling $v_t \propto d^2(\rho_{metal} - \rho_{slag})g/\mu$ may help interpret the sensitivity to size and viscosity (9). Industrial slags with solid particles, turbulence, reacting interfaces, droplet deformation, or coalescence may violate these assumptions. Report number-based and volume-weighted droplet-size distributions, and quantify the V mass contained in entrained inclusions rather than relying on a single average diameter.

Table 5 organizes the following synthesis to compare mechanisms and evidentiary requirements across the available studies.

**Table 5.** Differential diagnosis of vanadium losses and corresponding process responses.

| Loss pathway | Discriminating measurement | Conditional process response |
|---|---|---|
| V dissolved in oxidic slag. | Liquid-phase slag assay with phase-aware analysis | Reconsider $pO_2$, alloy capacity, and slag formulation |
| V incorporated in spinel or other crystals | XRD and quantitative SEM–EDS/EPMA phase mapping | Adjust composition and thermal path after phase-stability assessment |
| V in metallic droplets within slag | Polished-section imaging and recovered-inclusion assay | Improve coalescence, residence time, viscosity, and tapping |
| V in dust or wall deposits | Collected dust/deposit mass and V assay | Improve capture, accounting, and reactor handling |
| Apparent loss from sampling or closure error | Replicate assays and reconciled elemental balance | Correct inventory and analytical bias before modifying furnace conditions |

*Note.* Critical synthesis of the cited literature and methodological recommendations; no new experimental measurements are reported.

The diagnostic comparison in Table 5 prevents the same corrective action from addressing chemical retention and mechanical separation losses.

## 10. Critical Partitioning Assessment and Recovery Improvement Strategies

An evidence-based optimization sequence starts with closing the total V balance, followed by physically separating metal inclusions from oxide-bearing fractions, oxidation-

JIRRS
Journal International Review of Research Studies
**Received:** 13/06/2026 - **Accepted:** 07/11/2026
**Vol**: 1.11
**DOI**: 10.66104/dr86mq28
**Pages:** 1-34

state analysis, and equilibrium modeling. Figure 4 presents the decision framework. If chemical retention dominates, priority actions include modifying oxygen potential, temperature, slag composition, and alloy sink capacity. If mechanical entrainment dominates, priority shifts toward slag fluidity, coalescence and settling time, hydrodynamic control, and appropriate tapping practices.

Step 1 — Quantify feed and all outgoing V inventories, and evaluate closure and uncertainty.

Step 2 — Separate slag-bound V into liquid oxide, crystals, and entrained metal droplets using phase-aware sampling and microscopy.

Step 3 — Diagnose the dominant pathway: chemical oxide retention; phase crystallization; physical entrainment; or dust/deposit loss.

Step 4 — Select a mechanism-specific intervention: control $pO_2$ and slag/alloy activities; modify liquidus and crystallization; improve droplet settling/tapping; or capture dust and repair measurement gaps.

Step 5 — Repeat the mass balance and confirm improvement in recovered kg V per tonne dry feed.

**Figure 4.** Diagnosis-first workflow for phase-resolved V accounting and selection of mechanism-specific smelting interventions. Author-developed textual schematic based on the critical synthesis. Figure 4 is newly represented as an author-developed text schematic; no third-party graphical asset is included in this panel.

The workflow first establishes the V inventory and separates dissolved oxide-bound V from metal inclusions; only then does it direct changes to oxygen potential, slag formulation, or droplet-settling conditions.

The most comparable reporting basis includes V mass in each input and output stream (kg per batch or kg $h^{-1}$), phase-specific V concentrations (wt%), moles of reducible oxides, measured or modeled oxygen potential, liquid and solid phase fractions, viscosity at process temperature, alloy mass and composition, thermal history, and recovery uncertainty. Table 7 identifies the minimum evidence associated with each V-bearing destination.

Published recovery values should not be compared without normalizing these variables. A high initial alumina loading, for instance, may alter liquidus temperature and require a different flux balance from lower-alumina feeds. Similarly, iron, titanium, or

JIRRS
Journal International Review of Research Studies
**Received:** 13/06/2026 - **Accepted:** 07/11/2026
**Vol**: 1.11
**DOI**: 10.66104/dr86mq28
**Pages:** 1-34

chromium can alter the identity and amount of spinel-bearing phases. A process window optimized for a specific catalyst cannot be generalized without sensitivity analysis.

The most consequential knowledge gaps are equilibrium partition data for realistic Ni–Mo–V–Fe alloy/high-$Al_2O_3$ slag pairs; measured oxygen and carbon potentials; phase-resolved V analyses before and after quenching; experiments linking viscosity to alloy-droplet settling; and independently reconciled elemental balances with uncertainty estimates. Each proposed measurement addresses a distinct failure mode. These datasets would help determine whether recovery improvements are thermodynamic, kinetic, or due to physical separation, and would also support safer slag management.

Table 6 organizes the following synthesis to compare mechanisms and evidentiary requirements across the available studies.

**Table 6.** Minimum experimental reporting matrix for a transferable Ni–Mo–V smelting study.

| Reporting block | Minimum variables/outputs | Reason required |
|---|---|---|
| Feed and reagent inventory | Masses, elemental assays, moisture, reductant and flux additions | Defines a comparable input basis |
| Thermal/redox conditions | Temperature history, atmosphere, $pO_2$ or gas ratio, carbon activity if available | Constrains reduction and phase-stability interpretation |
| Phase-resolved products | Alloy/slag/dust mass and assays; dissolved/crystalline/entrained V fractions | Separates chemical and mechanical losses |
| Separation conditions | Hold time, droplet-size observations, viscosity and solids fraction where measured. | Explains differences between equilibrium and collected yield |
| Quality and uncertainty | Replicates, sampling method, closure residual and measurement uncertainty | Enables transparent inter-study comparison |

*Note.* Critical synthesis of the cited literature and methodological recommendations; no new experimental measurements are reported.

Table 6 converts the conceptual framework into a reporting checklist; not every listed measurement is available in the studies reviewed, which remains a limitation of cross-study synthesis.

**Table 7.** Phase-resolved evidence required for credible vanadium deportment assessment.

| Destination | Evidence/measurement | Interpretive limitation |
|---|---|---|
| Bulk alloy | Alloy mass; multielement assay; phase microanalysis | Bulk yield is not an equilibrium partition |

JIRRS
Journal International Review of Research Studies
**Received:** 13/06/2026 - **Accepted:** 07/11/2026
**Vol**: 1.11
**DOI**: 10.66104/dr86mq28
**Pages:** 1-34

| Destination | Evidence/measurement | Interpretive limitation |
|---|---|---|
| Oxide melt | Quenched slag plus phase separation; chemistry and thermodynamics | Quench crystallization can change measured phases |
| Spinel/crystals | XRD; SEM–EDS/EPMA; phase-fraction estimate | V-bearing crystals may form on cooling |
| Entrained droplets | Polished sections; imaging; liberated metal assay | Can be misclassified as slag-bound V |
| Dust/wall deposits | Collected dust and residue inventory | Often missing from reported closure |

## 11. Critical Synthesis Across Evidence Classes

### 11.1 Direct spent-catalyst smelting evidence

Class A provides the most directly applicable process evidence but does not isolate equilibrium properties from reactor-scale collection. Shi et al. (2023) demonstrated high V capture in a specially formulated high-$Al_2O_3$ slag at 1500 °C. Wang et al. (2023) demonstrated strongly different Ni/Mo/V recovery under reduction–sulfurization (25.1% V at 1450 °C) and a separately configured reduction-smelting route (89.7% V at 1525 °C). Their ferro-/aluminosilicate observations support direct investigation of the chemical association of retained V. Neither case measures a universal slag/metal partition coefficient. Differences in catalyst pretreatment, mixed feed, and flux additions prevent unqualified comparison.

### 11.2 Thermodynamic metal–slag analogs

Class B controlled Fe–slag equilibrations, including Wright and Davidson (2021), support sensitivity to oxygen potential, activity, and temperature. However, carbon-saturated Fe differs from Ni–Mo–V–Fe alloy in V chemical potential and sink capacity. Reported partition ratios must match the definition, reference state, liquid phase, temperature, carbon activity, and slag saturation before they can be used even for qualitative comparison. Class C steelmaking and other V-slag studies inform mechanisms rather than predict catalyst-smelting yields.

### 11.3 Crystalline vanadium retention and thermal reconstruction

Diao et al. (2016, 2018, 2024) and Lindvall et al. (2017) show why V-bearing spinel and other oxide-phase stability must be distinguished from the properties of a homogeneous liquid slag. A quenched crystal is not proof of high-temperature solid retention. Credible

JIRRS
Journal International Review of Research Studies
**Received:** 13/06/2026 - **Accepted:** 07/11/2026
**Vol**: 1.11
**DOI**: 10.66104/dr86mq28
**Pages:** 1-34

phase-specific deportment combines representative sampling, quantified phase mass, phase assay, and thermal-history constraints. Measured bulk slag V is chemically ambiguous without imaging of metallic droplets and identification of solid V phases.

### 11.4 Physical separation, slag transport and refractory interactions

Chemical oxide retention and metallic entrainment call for different optimizations. V-bearing metal droplets can be fully reduced yet fail to coalesce, settle or enter the tapped alloy. Liquid viscosity, liquidus margin, effective solids fraction, density difference, droplet-size distributions, turbulence and refractory compatibility interact. Slag fluidization must not be presented as intrinsically reducing oxide V solubility: an addition can simultaneously increase physical collection and stabilize a V-bearing oxide phase. The process objective is recovered elemental V mass, not minimum viscosity or minimum slag V concentration in isolation.

### 11.5 Alternative downstream routes and environmental boundaries

Roasting/leaching, selective hydrometallurgical recovery and post-smelting alloy oxidation-leaching provide alternative process boundaries and possible treatments for V-rich residual phases. They are not direct evidence of reductive-smelting alloy yield. Comparing these routes requires kg V recovered per tonne dry catalyst, energy and consumable burdens, dust and sulfur emissions, refractory wear, slag leachability and secondary waste. Broader reviews (Ying et al., 2025; Tian et al., 2026) position this article as a focused diagnostic synthesis rather than a general overview of spent-catalyst processing.

### 11.6 Evidence limitations and priorities

The principal gap is a calibrated dataset linking realistic Ni–Mo–V–Fe alloy chemistry and alumina-rich slags to measured oxygen potential, carbon and sulfur activities, high-temperature liquid/solid phase fractions, droplet-size-resolved entrainment, comprehensive V balances and replicate uncertainty. The evidence hierarchy matters: the numerical abundance of class B/C literature must not substitute for class A process validation. Pilot programs should explicitly test chemical retention versus metal collection before imposing additional reductant or modifying slag basicity.

JIRRS
Journal International Review of Research Studies
**Received:** 13/06/2026 - **Accepted:** 07/11/2026
**Vol**: 1.11
**DOI**: 10.66104/dr86mq28
**Pages:** 1-34

## 12. Conclusions

Vanadium recovery in reductive smelting of spent NiMoV catalysts cannot be inferred from nominal carbon addition, Ni/Mo recovery, or a bulk-slag V assay. Direct experiments demonstrate both high recovery and pronounced sensitivity to process configuration. The correct interpretation separates V collected in bulk alloy, dissolved in oxidic liquid, retained in crystalline oxides, present in entrained metal droplets, and transferred to dust or deposits. Phase-specific inventories and reconciled uncertainty must precede mechanistic claims.

Oxygen potential, alloy activities, the aluminosilicate support contribution, sulfur/FeO interactions, liquidus and solids fraction, thermal history, and droplet coalescence jointly determine the outcome. Available iron–slag analogs motivate thermodynamic hypotheses but cannot supply universal Ni–Mo–V partition coefficients. A diagnosis-first mass balance with clear feed and product mass bases offers the most actionable route to selective process interventions and more transferable pilot data.

## Declarations

### Funding

This review received no specific external funding.

### Conflict of Interest

The author declares no conflict of interest.

### Data Availability

No new experimental datasets were generated. The revised review discusses published evidence, accounting identities, and diagnostic recommendations. The author checked quantitative comparisons from Wang et al. (2023) against the original journal source; the author recommends final verification of remaining bibliographic records and quantitative statements before submission.

### Author Contributions

The author performed conceptualization, critical analysis, literature synthesis, visualization, and manuscript preparation.

## References

Amato, A., Ippolito, N. M., D'Arcangelo, M., Becci, A., Innocenzi, V., & Ferella, F. (2025). Vanadium, molybdenum and nickel: A sustainability analysis of the extraction from ores versus recovery from spent catalysts. Journal of Cleaner Production, 515, 145817. https://doi.org/10.1016/j.jclepro.2025.145817

JIRRS
Journal International Review of Research Studies

**Received:** 13/06/2026 - **Accepted:** 07/11/2026
**Vol**: 1.11
**DOI**: 10.66104/dr86mq28
**Pages:** 1-34

An, Y., Ma, B., Li, X., Chen, Y., Wang, C., Wang, B., Gao, M., & Feng, G. (2023). A review on the roasting-assisted leaching and recovery of V from vanadium slag. Process Safety and Environmental Protection, 173, 263–276. https://doi.org/10.1016/j.psep.2023.03.013

Andersson, A., Lee, M. J., Park, S. H., Hwang, S. M., Engström, F., & Park, J. H. (2026). The incorporation of $VO_x$ in the glass structure of electric arc furnace slag and its implication on slag valorization. Journal of Sustainable Metallurgy, 12, 3785–3801. https://doi.org/10.1007/s40831-026-01534-8

Aromaa-Stubb, R., Rinne, M. (2025). Life cycle assessment of Mo, V, Ni, and Co recovery from spent catalyst. ACS Sustainable Resource Management, 2(8), 1508–1516. https://doi.org/10.1021/acssusresmgt.5c00243

Chen, L., Wang, Z., Qin, Z., Zhang, G., Yue, H., Liang, B., & Luo, D. (2021). Investigation of the selective oxidation roasting of vanadium-iron spinel. Powder Technology, 387, 434–443. https://doi.org/10.1016/j.powtec.2021.04.009

Chen, R., Feng, C., Tan, J., Zhang, C., Yuan, S., Liu, M., Hu, H., Li, Q., & Hu, J. (2022). Stepwise separation and recovery of molybdenum, vanadium, and nickel from spent hydrogenation catalyst. Hydrometallurgy, 213, 105910. https://doi.org/10.1016/j.hydromet.2022.105910

Chen, Y., Wu, X., Guan, W., Xiao, S., Fang, K., Qing, J., Xie, R., Wu, S., Li, Q., Cao, Z., Wang, M., & Zhang, G. (2024a). Efficient recovery of all valuable metals from spent HDS catalysts: Based on roasting mechanisms for enhanced selective leaching and separation. Journal of Environmental Chemical Engineering, 12(5), 113485. https://doi.org/10.1016/j.jece.2024.113485

Chen, L., Wang, Z., Zhu, Y., Wu, K., Liang, B., & Luo, D. (2024b). Innovative strategy for comprehensive utilization of vanadium slag: Maximizing valuable metals recovery and minimizing hazardous waste generation. Process Safety and Environmental Protection, 188, 13–24. https://doi.org/10.1016/j.psep.2024.05.064

Chen, J., Sun, S., Xiao, F., & Tu, G. (2025). Advancing total management of oily spent hydroprocessing catalyst: From hazardous waste to circular and eco-sustainable utilization. Journal of Environmental Management, 381, 125202. https://doi.org/10.1016/j.jenvman.2025.125202

Cheng, J., Li, H.-Y., Wei, C.-C., Chen, X.-M., Diao, J., Xie, B., & Pan, F. (2024). Phase evolution mechanism exploration of vanadium slag during magnesiation roasting by atomic atmosphere method. Powder Technology. https://doi.org/10.1016/j.powtec.2024.119739

Cheng, J., Li, H.-Y., Gao, D.-B., Chen, X.-M., Hai, D., Diao, J., Xie, B., & Pan, F.-S. (2025a). Our journey in greenization of vanadium extraction from vanadium slag in China. Transactions of Nonferrous Metals Society of China, 35(4), 1306–1324. https://doi.org/10.1016/S1003-6326(24)66750-6

JIRRS
Journal International Review of Research Studies

**Received:** 13/06/2026 - **Accepted:** 07/11/2026
**Vol**: 1.11
**DOI**: 10.66104/dr86mq28
**Pages:** 1-34

Cheng, J., Li, H.-Y., Zhang, G.-W., Chen, X.-M., Diao, J., Xie, B., & Pan, F. (2025b). Understanding the atomic-scale evolution mechanism of V and Cr in V slag with high Cr content during magnesiation roasting toward tailing toxicity minimization. Process Safety and Environmental Protection, 194, 816–824. https://doi.org/10.1016/j.psep.2024.12.069

Deng, R., Xiao, H., Xie, Z., Liu, Z., Yu, Q., Chen, G., & Tao, C. (2020). A novel method for extracting vanadium by low-temperature sodium roasting from converter vanadium slag. Chinese Journal of Chemical Engineering, 28(8), 2208–2213. https://doi.org/10.1016/j.cjche.2020.03.038

Derensy, M., & Tonnesen, T. (2026a). Effect of vanadium-bearing slag aggregates on the microstructure and thermo-mechanical properties of alumina refractory castables. Materials, 19(5), 983. https://doi.org/10.3390/ma19050983

Derensy, M., & Tonnesen, T. (2026b). From metallurgical waste to sustainable refractory binder: Hydraulic performance of vanadium-bearing slags. Ceramics International, 52, 24261. https://doi.org/10.1016/j.ceramint.2026.03.464

Diao, J., Zhou, W., Gu, P., Ke, Z., Qiao, Y., & Xie, B. (2016). Competitive growth of crystals in vanadium–chromium slag. CrystEngComm, 18, 6272–6281. https://doi.org/10.1039/C6CE01087C

Diao, J., Shao, L., Zhou, W., Zhang, T., & Xie, B. (2018). Isothermal growth of spinel crystals in vanadium-chromium slag. Crystal Research and Technology, 53(3), 1700276. https://doi.org/10.1002/crat.201700276

Diao, J., Tao, H., Lai, Z., Qiu, Y., Chen, L., Li, H., & Xie, B. (2024). Crystallization behavior and growth mechanisms of spinel crystals in vanadium slag with high MgO content. CrystEngComm, 26, 2248. https://doi.org/10.1039/D4CE00189C

Ding, S., Liu, Y., Ma, B., Wang, K., Wang, C., & Chen, Y. (2026). Effective separation of vanadium and chromium from vanadium-chromium slag via sodium roasting-water leaching and solvent extraction. Minerals Engineering, 245, 110363. https://doi.org/10.1016/j.mineng.2026.110363

Drużyński, S., Wróbel-Kaszanek, A., Igliński, B., Kiełkowska, U., & Mazurek, K. (2026). Recovery of $V_2O_5$ from spent vanadium catalysts: Materials insights into deactivation and recycling strategies. Catalysts, 16(6), 522. https://doi.org/10.3390/catal16060522

Du, W.-T., Yao, T.-F., Cheng, H.-M., Ju, D.-C., & Chen, Z. (2024). Effects of spinel crystallization characteristics on leaching vanadium from vanadium-containing slag. Metallurgical and Materials Transactions B, 55, 4077. https://doi.org/10.1007/s11663-024-03239-3

Fan, X., Zhang, J., Zong, Y., Jiao, K., Zhang, Y., & Wu, H. (2026). Current advances in understanding the thermal stability of metallurgical slags. Metallurgical and Materials Transactions B, 57, 1327. https://doi.org/10.1007/s11663-025-03936-7

Fang, K., Zhang, G., Li, Q., Guan, W., Wang, M., Wu, S., Xia, X., & Shi, C. (2024). Efficient and selective recovery of Mo and V from spent hydrodesulfurization catalysts via

JIRRS
Journal International Review of Research Studies

**Received:** 13/06/2026 - **Accepted:** 07/11/2026
**Vol**: 1.11
**DOI**: 10.66104/dr86mq28
**Pages:** 1-34

oxidation roasting followed by $Na_2CO_3$ and NaOH leaching. Hydrometallurgy, 229, 106381. https://doi.org/10.1016/j.hydromet.2024.106381

Feng, C., Zhang, C., Yuan, S., Liu, M., Chen, R., Hu, H., & Hu, J. (2022). Sustainable recovery of surface-deposited oils and valuable metals from uncrushed spent hydroprocessing catalysts. Journal of Cleaner Production, 338, 130564. https://doi.org/10.1016/j.jclepro.2022.130564

Feng, C., Zhu, P., Zhang, L., Yu, J., Zheng, C., Luo, J., Tan, J., & Hu, J. (2024). Synchronous conversion and targeted separation of valuable metals from spent hydroprocessing catalysts. Journal of Cleaner Production, 479, 144064. https://doi.org/10.1016/j.jclepro.2024.144064

Feng, G., Gao, J., Lan, X., Guo, L., & Guo, Z. (2025a). A green and sustainable method for stepwise extraction of V and Ti from vanadium slag using super-gravity. Journal of Cleaner Production, 505, 145501. https://doi.org/10.1016/j.jclepro.2025.145501

Feng, G., Gao, J., Lan, X., Guo, L., & Guo, Z. (2025b). Enhanced separation of V-spinel and Ti-spinel in vanadium slag guided by crystallization mechanism. Journal of the American Ceramic Society, 108. https://doi.org/10.1111/jace.20701

Feng, G., Gao, J., Lan, X., Guo, L., & Guo, Z. (2025c). Phase diagrams of "FeO"–$SiO_2$–CaO–$V_2O_3$–$TiO_2$ system and phase transformation of vanadium-enriched phases. ISIJ International, 65(12), 1850–1859. https://doi.org/10.2355/isijinternational.ISIJINT-2025-086

Gan, H., Zhao, B., Liu, Q., He, X., Shi, Z., Han, S., Li, K., Liu, B., Zhang, S., & Ding, Y. (2026). Critical reviews on recovery of valuable metals from spent petroleum catalysts. Separation and Purification Technology, 392, 137206. https://doi.org/10.1016/j.seppur.2026.137206

Gao, J., Lu, W., Li, Y., & Wu, T. (2024). Organic acid-mediated leaching kinetics study and selective extraction of Mo, V, and Ni from spent catalysts. Waste Management, 187, 198–206. https://doi.org/10.1016/j.wasman.2024.07.022

Guo, Z., Chen, X., Shi, Y., Zhu, D., Pan, J., Yang, C., Li, S., Xu, J., & Wang, X. (2025). Smelting separation behaviors of various reduced vanadium titanomagnetite pellets. Transactions of Nonferrous Metals Society of China, 35(11), 3869–3885. https://doi.org/10.1016/S1003-6326(25)66918-4

Guo, Z., Chen, X., Zhu, D., Pan, J., Yang, C., & Li, S. (2026). Integrated valorization of vanadium–titanium magnetite for recovery of vanadium-bearing molten iron and rutile-rich $TiO_2$ product. Metals, 16(8), 888. https://doi.org/10.3390/met16080888

Han, Y., Kim, S., Go, B., Lee, S., Park, S., & Jeon, H.-S. (2021). Optimized magnetic separation for efficient recovery of V- and Ti-enriched concentrates from vanadium-titanium magnetite ore: Effect of grinding and magnetic intensity. Powder Technology, 391, 282–291. https://doi.org/10.1016/j.powtec.2021.06.024

Han, Y., Chen, J., Deng, Y., Liu, T., & Li, H. (2023). A leaching, solvent extraction, stripping, precipitation, and calcination process for the recovery of $MoO_3$ and NiO

JIRRS
Journal International Review of Research Studies

**Received:** 13/06/2026 - **Accepted:** 07/11/2026
**Vol**: 1.11
**DOI**: 10.66104/dr86mq28
**Pages:** 1-34

from spent hydrofining catalysts. Hydrometallurgy, 106046. https://doi.org/10.1016/j.hydromet.2023.106046

He, Z., Liu, J., Yang, S., Yang, H., & Xue, X. (2016). Partition of valuable components between slag and metal in the blast furnace operating with high chromium, vanadium, titanium, magnetite ores. Metallurgical Research & Technology, 113(6), 607. https://doi.org/10.1051/metal/2016041

He, Y., Zhang, J., Li, W., Huo, X., Li, H., Guo, M., & Zhang, M. (2026). Triple synergy by one-step reductive smelting separation for full utilization of vanadium extraction tailings: Detoxification, Fe-Cr-V wear-resistant alloy preparation and co-production of Ti-rich residue. Journal of Hazardous Materials, 514, 142649. https://doi.org/10.1016/j.jhazmat.2026.142649

Heo, J., Lee, Y., Park, H., & Park, J. H. (2021). Influence of slag composition and oxygen potential on thermodynamic behavior of vanadium in $FeO–TiO_2–MgO–SiO_2–Al_2O_3$ smelting slag and molten iron. Journal of Materials Research and Technology, 15, 5723–5732. https://doi.org/10.1016/j.jmrt.2021.11.035

Hu, Q., Ma, D., Zhou, K., Liu, Y., You, Y., You, Z., & Lv, X. (2022). Phase transformation and slag evolution of vanadium–titanium magnetite pellets during softening–melting process. Powder Technology, 396, 710–717. https://doi.org/10.1016/j.powtec.2021.11.035

Hu, P., Zhang, Y., Liu, H., Liu, T., Li, S., Zhang, R., & Guo, Z. (2023a). Highly efficient vanadium extraction from vanadium slag using an enhanced acid leaching-coprecipitation process. Separation and Purification Technology, 304, 122319. https://doi.org/10.1016/j.seppur.2022.122319

Hu, Q., Pan, S., Gao, X., Liu, Y., Huang, Q., You, Y., You, Z., & Lv, X. (2023b). Selective nitridation–corrosion process to recover vanadium, titanium, chromium, and iron from vanadium slag. Journal of Environmental Management, 325, 116604. https://doi.org/10.1016/j.jenvman.2022.116604

Hua, Q., Ma, J., Xu, P., Zhang, S., Rong, J., & Chen, Z. (2025). Hydrothermal acid leaching process with ultra-high efficiency for vanadium from spent catalyst. Minerals Engineering, 234, 109777. https://doi.org/10.1016/j.mineng.2025.109777

Huang, W., & Liu, Y. (2020). Crystallization behavior and growth mechanisms of spinel crystals in vanadium-containing slags. ISIJ International, 60(10), 2183–2190. https://doi.org/10.2355/isijinternational.ISIJINT-2020-039

Jantzen, T., Yazhenskikh, E., Hack, K., Baben, M., Wu, G., & Müller, M. (2021). Addition of $V_2O_5$ and $V_2O_3$ to the $CaO–FeO–Fe_2O_3–MgO–SiO_2$ database for vanadium distribution and viscosity calculations. Calphad, 74, 102284. https://doi.org/10.1016/j.calphad.2021.102284

Jia, Y., Qing, Y., Feng, B., Zhong, Y., Dai, L., & Wang, M. (2024). Green redox separation and efficient extraction of vanadium and chromium from leaching solution of chrome-

JIRRS
Journal International Review of Research Studies

**Received:** 13/06/2026 - **Accepted:** 07/11/2026
**Vol**: 1.11
**DOI**: 10.66104/dr86mq28
**Pages:** 1-34

vanadium slag. Separation and Purification Technology, 127098. https://doi.org/10.1016/j.seppur.2024.127098

Jiang, T., Wen, J., Zhou, M., & Xue, X. (2018). Phase evolutions, microstructure and reaction mechanism during calcination roasting of high chromium vanadium slag. Journal of Alloys and Compounds, 742, 402–412. https://doi.org/10.1016/j.jallcom.2018.01.201

Jing, J.-F., Wang, S., Guo, Y.-F., Chen, F., Zhang, J., Yang, L.-Z., & Qiu, G.-Z. (2026a). Anosovite-dominated slag design for Fe-V-Ti separation in electric-furnace smelting of vanadium titanomagnetite. Journal of Materials Research and Technology, 45, 1624–1635. https://doi.org/10.1016/j.jmrt.2026.09.175

Jing, J.-F., Guo, Y.-F., Wang, S., Chen, F., Yang, L.-Z., & Qiu, G.-Z. (2026b). Phase composition of slag–iron interface and elemental distribution behavior between hot metal and Ti-bearing electric furnace slags. Transactions of Nonferrous Metals Society of China, 36(4), 1320–1334. https://doi.org/10.1016/S1003-6326(25)67033-6

Li, X., Ni, P., Deng, T., Hou, X., Gao, W., & Li, Y. (2024a). A novel process for recovery of vanadium and chromium from vanadium-chromium sludge: Roasting pretreatment and thermal reduction co-alloying process. Journal of Cleaner Production, 483, 144275. https://doi.org/10.1016/j.jclepro.2024.144275

Li, J., Diao, J., Lai, Z., Hu, R., Tan, W., Chen, L., Li, H., & Xie, B. (2024b). Corrosion of MgO–C refractories by vanadium slag with high MgO content. Ceramics International, 50(17), 31147–31153. https://doi.org/10.1016/j.ceramint.2024.05.420

Li, Q., Gu, S., Yu, L., Zhang, L., Dong, J., Jia, J., & Li, C. (2024c). Green method for preparing $NaVO_2$ from vanadium-chromium slag based on $Na_2CO_3$ roasting and water leaching. Journal of Environmental Chemical Engineering, 12(6), 114834. https://doi.org/10.1016/j.jece.2024.114834

Li, C., Jiang, T., Wen, J., Yu, T., & Li, F. (2024d). Review of leaching, separation, and recovery of vanadium from roasted products of vanadium slag. Hydrometallurgy, 226, 106313. https://doi.org/10.1016/j.hydromet.2024.106313

Li, Q., Gu, S., Yu, L., Han, F., & Dong, J. (2024e). Separation of vanadium and chromium from vanadium-chromium slag by high-temperature heating. Separation and Purification Technology, 336, 126098. https://doi.org/10.1016/j.seppur.2023.126098

Li, C., An, X., Jiang, T., Wen, J., Hao, G., Yang, G., Yu, T., Zhang, L., & Liu, X. (2025a). Cleaner and efficient vanadium extraction from vanadium slag: Optimal adaptation mechanism between calcination roasting and reductive leaching processes. Journal of Cleaner Production, 527, 146598. https://doi.org/10.1016/j.jclepro.2025.146598

Li, C., An, X., Jiang, T., & Wen, J. (2025b). Efficient recovery of vanadium from calcified vanadium slag by reductive leaching-selective precipitation: Thermodynamic and kinetic analysis and mechanism investigation. Separation and Purification Technology, 134009. https://doi.org/10.1016/j.seppur.2025.134009

Li, J., Tang, K., Chen, Y., Ma, Y., Zhang, Q., Liu, Z., Tao, C., Peng, Y., Du, J., Xie, Z., He, W., & Shen, B. (2025c). Metastable phase reconstruction for enhanced vanadium

JIRRS
Journal International Review of Research Studies

**Received:** 13/06/2026 - **Accepted:** 07/11/2026
**Vol**: 1.11
**DOI**: 10.66104/dr86mq28
**Pages:** 1-34

extraction via cerium oxide-catalyzed low-sodium roasting. Journal of Cleaner Production, 145380. https://doi.org/10.1016/j.jclepro.2025.145380

Li, C., Jiang, T., Wen, J., An, X., Hao, G., Zhang, L., Yu, T., & Yang, G. (2026). Sustainable recovery of vanadium from vanadium slag via low-entropy phase reconstruction and reduction-mediated method. Chemical Engineering Journal. https://doi.org/10.1016/j.cej.2026.178534

Liang, X., Tang, J., Li, L., Wu, Y., & Sun, Y. (2022). A review of metallurgical processes and purification techniques for recovering Mo, V, Ni, Co, Al from spent catalysts. Journal of Cleaner Production, 376, 134108. https://doi.org/10.1016/j.jclepro.2022.134108

Lindvall, M., Berg, M., & Sichen, D. (2017a). The effect of $Al_2O_3$, CaO, and $SiO_2$ on the phase relationship in FeO–$SiO_2$-based slag with 20 mass% vanadium. Journal of Sustainable Metallurgy, 3, 289–299. https://doi.org/10.1007/s40831-016-0088-y

Lindvall, M., Tikka, J., Berg, M., Ye, G., & Sichen, D. (2017b). Vanadium extraction from a Fe–V (2.0 mass%)–P (0.1 mass%) melt and investigation of the phase relations in the formed FeO–$SiO_2$-based slag with 20 mass% V. Journal of Sustainable Metallurgy, 3, 808–822. https://doi.org/10.1007/s40831-017-0147-z

Liu, D., Diao, J., Wang, G., & Xie, B. (2019). Analysis of V and Cr with various valence states in FeO–$SiO_2$–MnO–$TiO_2$–$VO_x$–MgO–$CrO_x$ system by XPS method. Metallurgical Research & Technology, 116(2). https://doi.org/10.1051/metal/2018075

Liu, S., Wang, L., & Chou, K.-C. (2021). Innovative method for minimization of waste containing Fe, Mn, and Ti during comprehensive utilization of vanadium slag. Waste Management, 127, 179–188. https://doi.org/10.1016/j.wasman.2021.04.034

Liu, S., Wang, L., Chen, J., Ye, L., & Du, J. (2024). Research progress of vanadium extraction processes from vanadium slag: A review. Separation and Purification Technology, 342, 127035. https://doi.org/10.1016/j.seppur.2024.127035

Liu, H., Wang, X., Zhang, W., Wen, J., Wang, J., Ye, J., Zhan, Y., Huang, G., & Xu, S. (2025a). Acid-free process for selective and efficient recovery of molybdenum from spent hydrodesulfurization catalysts. Journal of Environmental Management, 380, 125029. https://doi.org/10.1016/j.jenvman.2025.125029

Liu, X., Sun, Y., Wen, J., Jiang, T., Zhang, L., Yang, J., & Dai, J. (2025b). Green extraction of vanadium resources: A process for the preparation of vanadium oxide in an ammonia-free system. Chinese Journal of Chemical Engineering, 88, 265–273. https://doi.org/10.1016/j.cjche.2025.07.007

Ma, J.-F., Wang, G.-W., Zhang, J.-L., Liu, Z.-J., Jiao, K.-X., Guo, J., & Li, X.-Y. (2017). Reduction behavior and kinetics of vanadium–titanium sinters under high-potential oxygen-enriched pulverized coal injection. International Journal of Minerals, Metallurgy and Materials, 24, 493–503. https://doi.org/10.1007/s12613-017-1430-5

Madej, P., Czech, A., Pęcak, K., & Cybulski, A. (2025). Studies on removal of petroleum fractions from spent petrochemical catalysts to prepare them for pyrometallurgical

JIRRS
Journal International Review of Research Studies

**Received:** 13/06/2026 - **Accepted:** 07/11/2026
**Vol**: 1.11
**DOI**: 10.66104/dr86mq28
**Pages:** 1-34

recovery of Ni, Mo, and V. Scientific Reports, 15, 8837. https://doi.org/10.1038/s41598-025-91247-x

Mendoza, S., Garlick, C., Singh, T., Nusheh, M., Yin, B. H., Honeyands, T., & Bumby, C. W. (2026). Melting behavior of hydrogen-reduced vanadium-bearing titanomagnetite ironsand pellets in a laboratory-scale electrode smelter. Journal of Sustainable Metallurgy, 12, 1176–1188. https://doi.org/10.1007/s40831-025-01389-5

Neubert, L., Shyrokykh, T., Tinkova, N., Seetharaman, S., & Volkova, O. (2025). Extraction of vanadium from $CaO–SiO_2–MgO–Al_2O_3$ slags based on vaporization of vanadium pentoxide. Steel Research International, 96(8), 2300681. https://doi.org/10.1002/srin.202300681

Park, D., & Morita, K. (2026). Investigation of the thermodynamic properties of vanadium oxides in the $CaO–VO_x–Al_2O_3–SiO_2$ slag at 1873 K. Metallurgical and Materials Transactions B, 57, 869–879. https://doi.org/10.1007/s11663-025-03892-2

Pathak, A., Rana, M. S., Al-Sheeha, H., Navvamani, R., & Al-Sairafi, S. (2025). Sustainable extraction of valuable metals from petroleum spent hydroprocessing catalysts using a biodegradable lixiviant. Separation and Purification Technology, 128686. https://doi.org/10.1016/j.seppur.2024.128686

Peng, H. (2019). A literature review on leaching and recovery of vanadium. Journal of Environmental Chemical Engineering, 7(5), 103313. https://doi.org/10.1016/j.jece.2019.103313

Pereira, A. C. (2026a). Alloy nucleation, coalescence, and settling in Ni–Mo–V smelting: A critical review. Journal International Review of Research Studies, 1(7). https://doi.org/10.66104/p3c1fk38

Pereira, A. C. (2026b). From Vanadium–Titanium Magnetite to Fe–C–V Alloys: A Critical Review of Vanadium-Bearing Pig Iron Production, Vanadium Partitioning, Refining, and Metallurgical Applications. Journal International Review of Research Studies, 1(09 - September), 1–48. https://doi.org/10.66104/qa1tk476

Pereira, A. C. (2026c). Liquid-metal droplet coalescence in metallurgical slags: A critical review of interfacial phenomena, slag properties, hydrodynamics, kinetics, and metal recovery. International Journal of Research and Innovation in Social Science, 10(7), 15007–15036. https://doi.org/10.47772/IJRISS.2026.100701023

Pereira, A. C. (2026d). Recovery and recycling of spent Ni–Mo–V catalysts: Technologies, environmental drivers and circular economy perspectives. IKR Journal of Multidisciplinary Studies, 2, 41–64. https://doi.org/10.5281/zenodo.18838023

Pereira, A. C. (2026e). Slag composition control indices in high-temperature metallurgy: A critical review of viscosity, conductivity, corrosion, and refractory wear. Journal International Review of Research Studies, 1(4). https://doi.org/10.66104/7x5etg23

Qiu, Y., Sun, Y., Han, Y., & Gao, P. (2026). Advances in vanadium recovery from basic oxygen furnace vanadium slag: Mechanisms, extraction technologies, and emerging

JIRRS
Journal International Review of Research Studies

**Received:** 13/06/2026 - **Accepted:** 07/11/2026
**Vol**: 1.11
**DOI**: 10.66104/dr86mq28
**Pages:** 1-34

strategies. Journal of Environmental Chemical Engineering. https://doi.org/10.1016/j.jece.2026.121965

Renno, A. D., Möckel, R., Frenzel, M., Ebert, D., Bachmann, K., Krause, J., & Gutzmer, J. (2023). Metal deportment in complex secondary raw materials: The case of vanadium in basic oxygen furnace slags. Mining, Metallurgy & Exploration, 40, 2139–2152. https://doi.org/10.1007/s42461-023-00851-w

Rui, G., Guo, H., Chen, D., Wang, Z., Liu, S., Du, E., & Mao, L. (2025). Stepwise recycling of Mo and V from spent HDS catalysts by water–vapor-enhanced sublimation and $H_2O_2$ leaching process. Separation and Purification Technology, 379, 134861. https://doi.org/10.1016/j.seppur.2025.134861

Safari, H., Abdollahi, H., Ghassa, S., Rezaei, A., & Ghorbani, Y. (2026). Eco-friendly two-step leaching of molybdenum and nickel from spent hydrodesulfurization catalysts using glycine and alkaline solutions. Journal of Environmental Management, 397, 128219. https://doi.org/10.1016/j.jenvman.2025.128219

Shao, L., Diao, J., Zhou, W., Zhang, T., & Xie, B. (2019). Non-isothermal crystallization behavior of spinel crystals in $FeO–SiO_2–TiO_2–V_2O_3–Cr_2O_3$ slag. Metallurgical Research & Technology, 116(1), 110. https://doi.org/10.1051/metal/2018033

Shao, J., Sun, X., He, Y., Zhao, Y., Chen, S., & Liang, F. (2025). Thermodynamic and kinetic analysis for phase transition of vanadium slag by calcined roasting. Mining and Metallurgical Engineering, 45(1), 103–108. https://doi.org/10.3969/j.issn.0253-6099.2025.01.019

Sharma, S. K., Girdwood, M. L., Arif, T., Pearcy, A. C., Tiffin, C. M., Marshall, A. T., & Bumby, C. W. (2025). Understanding the effect of roasting on vanadium speciation in steel slags and impact on leaching. Hydrometallurgy, 232, 106433. https://doi.org/10.1016/j.hydromet.2024.106433

Shi, Z.-S., Ding, Y.-J., Yin, X.-P., Liu, B., Shen, H.-L., Wu, B.-Y., Zhao, B.-H., Han, F.-L., Ekberg, C., & Zhang, S.-G. (2023). Enrichment of Ni–Mo–V via pyrometallurgical reduction from spent hydrogenation catalysts and the multi-reaction mechanism. Rare Metals, 42, 2700–2712. https://doi.org/10.1007/s12598-023-02278-0

Shi, Z., Ding, Y., Ren, J., He, X., Zhao, B., Zhong, J., Zhu, Y., Wang, B., & Zhang, S. (2024). Oxidation leaching of NiMoV alloy enriched from spent hydrogenation catalysts and solvent extraction of Mo and V. Journal of Environmental Chemical Engineering, 12(1), 111714. https://doi.org/10.1016/j.jece.2023.111714

Shi, C., Liu, Y., Urata, K., Yasui, S., Abe, T., & Kobayashi, Y. (2025). Thermodynamic investigation of MnAl2O4 spinel precipitation behavior in manganese-containing slag systems. ISIJ International, 65(13), 2269–2274. https://doi.org/10.2355/isijinternational.ISIJINT-2025-334

Singh, N., Jyothi, R. K., Pasupuleti, K. S., & Lee, J.-Y. (2025). Recovery of aluminum, vanadium, and nickel from waste desulfurization catalyst residue by roasting and

JIRRS
Journal International Review of Research Studies

**Received:** 13/06/2026 - **Accepted:** 07/11/2026
**Vol**: 1.11
**DOI**: 10.66104/dr86mq28
**Pages:** 1-34

water leaching. Journal of Industrial and Engineering Chemistry, 143, 632–644. https://doi.org/10.1016/j.jiec.2024.09.011

Sun, S., Yang, K., Liu, C., Tu, G., & Xiao, F. (2024). Recovery of nickel and preparation of ferronickel alloy from spent petroleum catalyst via cooperative smelting-vitrification process with coal fly ash. Environmental Technology, 45(11), 2108–2118. https://doi.org/10.1080/09593330.2021.2002421

Tang, K., Zhong, H., Chen, Y., Li, J., Du, J., Liu, Z., Liu, R., & Tao, C. (2025). Manganese-promoted sodium roasting and electric field-assisted leaching of vanadium slag for enhanced vanadium extraction. Journal of Industrial and Engineering Chemistry, 151, 556–564. https://doi.org/10.1016/j.jiec.2025.04.027

Tang, K., Li, J., Zhong, H., He, W., Du, J., Liu, R., Tao, C., & Chen, Y. (2026a). Deciphering phase reconstruction and element-specific migration pathways in vanadium slag spinel during multi-stage oxidative decomposition. Journal of Industrial and Engineering Chemistry, Advance online publication. https://doi.org/10.1016/j.jiec.2026.07.032

Tang, K., Li, J., Chen, Y., Zhong, H., Du, J., Liu, R., & Tao, C. (2026b). Efficient conversion of vanadium by calcium roasting: Mechanistic insights through tracking vanadium phase evolution. Journal of Industrial and Engineering Chemistry, 157, 561–574. https://doi.org/10.1016/j.jiec.2025.10.030

Taz, D., Ozsarac, S., Kursunoglu, S., Kursunoglu, N., Top, S., & Altiner, M. (2024). A review on the recovery of high-grade critical metals from spent petroleum catalysts for meeting the demands of Industry 5.0. Energy Sources, Part A: Recovery, Utilization, and Environmental Effects, 46(1), 4593–4607. https://doi.org/10.1080/15567036.2024.2332465

Tian, C., Gao, Y., Zhao, W., Ling, Z., Li, Z., Xie, H., & Mao, B. (2026). Recovery of valuable metals from spent HDS catalysts and comprehensive utilization of spent HDS. Separations, 13(8), 218. https://doi.org/10.3390/separations13080218

Vickerfält, A., Huss, J., Martinsson, J., & Sichen, D. (2023). Reaction mechanisms during melting of H-DRI focusing on slag formation and the behavior of vanadium. Metallurgical and Materials Transactions B, 54, 2206–2215. https://doi.org/10.1007/s11663-023-02827-z

Wang, Z., Chen, L., Aldahrib, T., Li, C., Liu, W., Zhang, G., Yang, Y., & Luo, D. (2020). Direct recovery of low-valence vanadium from vanadium slag—Effect of roasting on vanadium leaching. Hydrometallurgy, 191, 105156. https://doi.org/10.1016/j.hydromet.2019.105156

Wang, Z., Qin, Z., Chen, L., Liang, B., Zhu, Y., Wu, K., & Luo, D. (2023). Recovery of low-valence vanadium from vanadium slag for the preparation of VOSO4 electrolyte. Process Safety and Environmental Protection, 174, 298–309. https://doi.org/10.1016/j.psep.2023.03.040

JIRRS
Journal International Review of Research Studies

**Received:** 13/06/2026 - **Accepted:** 07/11/2026
**Vol**: 1.11
**DOI**: 10.66104/dr86mq28
**Pages:** 1-34

Wang, Y.-H., Wang, Y.-F., Li, Y.-T., Wu, C., Han, X.-L., Zhao, N.-N., Zhang, Z.-K., Dai, L., Wang, L., & He, Z.-X. (2024). A review on vanadium extraction techniques from major vanadium-containing resources. Rare Metals, 43(9), 4115–4131. https://doi.org/10.1007/s12598-024-02721-w

Wang, K., Ma, B., Liu, Y., Wang, C., & Chen, Y. (2025a). A novel method for vanadium recovery from Cr-rich vanadium slag via alkali leaching. Minerals Engineering, 232, 109559. https://doi.org/10.1016/j.mineng.2025.109559

Wang, Z.-H., Chen, S.-Y., Chen, L., Liang, B., & Luo, D.-M. (2025b). Enhancing iron and titanium recovery efficiency via coal-based direct reduction of vanadium-titanium magnetite raw ore. Transactions of Nonferrous Metals Society of China, 35(10), 3480–3492. https://doi.org/10.1016/S1003-6326(25)66894-4

Wang, D., Zhang, L., Li, J., Chen, C., Lin, Y., Yang, Z., Wang, D., Hou, H., Chen, J., Zhou, T., & Tang, W. (2025c). Separation and recovery of vanadium from leaching solution of calcium roasting vanadium slag by extraction with P204 extractant. Minerals Engineering, 232, 109540. https://doi.org/10.1016/j.mineng.2025.109540

Wang, W., Shi, Z., Yuan, C., Ma, B., Sun, G., & Liu, G. (2026). Recycling of Mo and V from spent hydrogenation catalysts via a one-step soda-roasting process. ACS Omega, 11(30), 44887–44902. https://doi.org/10.1021/acsomega.6c02148

Wang, Z., Wang, H., Jie, X., Zhao, X., Waters, K. E., Northwood, D. O., Cui, S., & Ma, H. (2023). Reduction–sulfurization smelting process of waste hydrogenation catalysts, automotive exhaust purifier waste catalysts, and laterite nickel ore. ACS Omega, 8(43), 40713–40728. https://doi.org/10.1021/acsomega.3c05772

Wen, J., Jiang, T., Yu, T., Chen, B., & Li, L. (2022a). Clean and efficient extraction of vanadium from vanadium slag: Effect of manganese on the phase composition and vanadium extraction process. Journal of Cleaner Production, 367, 133077. https://doi.org/10.1016/j.jclepro.2022.133077

Wen, J., Yu, T., Jiang, T., Sun, H., Li, M., & Peng, Y. (2022b). Effect of chromium content on the phase composition, crystallization, and component extraction of vanadium slag. Process Safety and Environmental Protection, 165, 13–21. https://doi.org/10.1016/j.psep.2022.06.031

Wen, J., Jiang, T., Sun, H., Yu, T., Li, M., & Peng, Y. (2022c). Investigation of the separation principle of vanadium and chromium in the Fe2VO4-CaO-FeCr2O4 system: Simplifying and simulating the calcination roasting process of vanadium-chromium slag. Journal of Industrial and Engineering Chemistry, 115, 378–389. https://doi.org/10.1016/j.jiec.2022.08.022

Wen, J., Jiang, T., Liu, M., Arken, S., Sun, H., Yu, T., & Chen, B. (2024). Observations and simulations for the separation mechanism of vanadium and chromium: Progressive study based on oxides, spinels, and vanadium-chromium slag. Journal of Environmental Chemical Engineering, 12(3), 112592. https://doi.org/10.1016/j.jece.2024.112592

JIRRS
Journal International Review of Research Studies

**Received:** 13/06/2026 - **Accepted:** 07/11/2026
**Vol**: 1.11
**DOI**: 10.66104/dr86mq28
**Pages:** 1-34

Wright, S., & Davidson, R. (2021). Distribution of vanadium between $Al_2O_3$–CaO–MgO–$SiO_2$–$TiO_2$ slag and carbon-saturated iron. Mineral Processing and Extractive Metallurgy, 130(4), 302–312. https://doi.org/10.1080/25726641.2019.1633505

Wu, L., Qi, C., Yan, B., Wang, J., & Dong, Y. (2020). Effect of alumina on the behavior of V-rich spinel phase in CaO–$SiO_2$–$FeO_t$–MgO–$Al_2O_3$–$V_2O_3$–$P_2O_5$ slags at 1573 K (1300 °C). Metallurgical and Materials Transactions B, 51(5), 2339–2347. https://doi.org/10.1007/s11663-020-01904-x

Wu, S., Jia, J., Yu, L., Zhang, L., Dong, J., & Li, C. (2026a). Impact of roasting on the acid leaching efficiency of valuable elements from vanadium slag. Minerals Engineering, 245, 110318. https://doi.org/10.1016/j.mineng.2026.110318

Wu, H., Qin, Y., Yu, X., Cheng, G., Xue, X., Du, H., & Liu, B. (2026b). Recycling of vanadium-extraction tailings by controllable aluminothermic reduction process. Journal of Cleaner Production, 571, 148759. https://doi.org/10.1016/j.jclepro.2026.148759

Wunderlich, S., Hampel, S., Ferreira Sanchez, D., Schirmer, T., & Fittschen, U. E. A. (2025). A microfocus study on basic-oxygen-furnace slag thin sections to understand the principles of vanadium incorporation. Journal of Synchrotron Radiation, 32(4), 986–993. https://doi.org/10.1107/S1600577525003868

Xiang, J., Wang, X., Pei, G., Huang, Q., & Lü, X. (2020). Recovery of vanadium from vanadium slag by composite roasting with CaO/MgO and leaching. Transactions of Nonferrous Metals Society of China, 30(11), 3114–3123. https://doi.org/10.1016/S1003-6326(20)65447-4

Xiong, Y., Wang, L., Wang, L., Li, S., Yang, G., Cao, C., Liu, S., Nie, Y., & Jia, L. (2023). Optimization and kinetic analysis of direct acid leaching of vanadium from converter vanadium slag under atmospheric pressure. Minerals Engineering, 198, 108091. https://doi.org/10.1016/j.mineng.2023.108091

Xu, G., Wang, J., Xu, F., Huang, G., Xu, S., & Wu, B. (2025). Highly efficient recovery of total components from spent hydroprocessing catalysts (HPCs) with minimal $CO_2$ & $SO_2$ emissions. Journal of Environmental Management, 375, 124204. https://doi.org/10.1016/j.jenvman.2025.124204

Xu, H., Yu, L., Ma, Z., Fang, S., Rao, S., Wang, D., Duan, L., Cao, H., & Liu, Z. (2026). Selective recovery of vanadium, molybdenum, and nickel from full-particle spent hydrodesulfurization catalysts via microwave roasting-ammonia leaching. Journal of Environmental Chemical Engineering, 14(5), 123633. https://doi.org/10.1016/j.jece.2026.123633

Yan, Z., Zheng, S., & Zhang, Y. (2025). Effects of vanadium valences on the solubility in $Fe_2TiO_5$ for helping to understand calcination roasting of vanadium slag. International Journal of Minerals, Metallurgy and Materials, 32, 2920–2929. https://doi.org/10.1007/s12613-025-3184-9

JIRRS
Journal International Review of Research Studies

**Received:** 13/06/2026 - **Accepted:** 07/11/2026
**Vol**: 1.11
**DOI**: 10.66104/dr86mq28
**Pages:** 1-34

Yao, Z., Zhang, Q., Wang, L., Zhang, W., Ma, B., & Wang, C. (2023). Non-salt roasting mechanism of V–Cr slag toward efficient selective extraction of vanadium. Journal of Industrial and Engineering Chemistry, 126, 588–600. https://doi.org/10.1016/j.jiec.2023.06.050

Ye, G., Zhang, Y., Xie, Y., Xiang, X., Rong, Y., & Song, C. (2025). A novel pretreatment process for vanadium extraction: Purification and recovery of negative component calcium in vanadium-bearing steel slag. Process Safety and Environmental Protection, 195, 106785. https://doi.org/10.1016/j.psep.2025.106785

Ying, Z., Chen, J., Shang, Z., Liu, T., Xu, S., & Wu, G. (2025). Recovery and resource utilization of spent hydrogenation catalysts: A review. Environmental Science & Technology, 59(29), 14809–14831. https://doi.org/10.1021/acs.est.5c04246

Yu, J., Ma, B., Zhao, S., Yao, Z., Wang, C., Wang, B., Gao, M., & Feng, G. (2023). Vanadium extraction from water-cooled vanadium converter slag via salt-free roasting and acid leaching. Process Safety and Environmental Protection, 172, 727–737. https://doi.org/10.1016/j.psep.2023.02.071

Yu, H., Liu, C., Liu, S., Gu, Y., Wang, S., Yaraş, A., Hu, L., Zhang, W., Peng, M., Arslanoğlu, H., & Mao, L. (2024). High-efficiency recycling of Mo and Ni from spent HDS catalysts: Enhanced oxidation with $O_2$-rich roasting and selective separation with organic acid leaching–complexation extraction. Journal of Hazardous Materials, 464, 132982. https://doi.org/10.1016/j.jhazmat.2023.132982

Yu, C.-C., Diao, J., Wang, J.-A., Tan, W.-F., Li, H.-Y., & Xie, B. (2025a). Effect of CaO and $P_2O_5$ on non-isothermal crystallization of alkaline vanadium slag. Transactions of Nonferrous Metals Society of China, 35(6), 2061–2073. https://doi.org/10.1016/S1003-6326(25)66801-4

Yu, T., Jiang, T., Wen, J., Zhang, L., Li, Y., Yang, X., & Yang, G. (2025b). Effect of ferromagnetic mineral on vanadium extraction from calcified vanadium slag. Minerals Engineering, 233, 109655. https://doi.org/10.1016/j.mineng.2025.109655

Yu, H., Liu, S., Yaraş, A., Enkhchimeg, B., Hu, L., Zhang, W., Peng, M., Arslanoğlu, H., & Mao, L. (2025c). Recovery of valuable metals from spent hydrodesulfurization (HDS) catalysts: A comprehensive research review and specific industrial cases. Journal of Environmental Management, 379, 124920. https://doi.org/10.1016/j.jenvman.2025.124920

Yue, H.-R., Zhao, Y.-K., Xue, X.-X., & Liu, J. (2025). Vanadium recovery with barium slag as a roasting additive: A novel waste-to-value approach. Journal of Cleaner Production, 506, 145470. https://doi.org/10.1016/j.jclepro.2025.145470

Zhang, B., Liu, C., Liu, Z., Li, Z., & Jiang, M. (2019). Remediation of the vanadium slag processing residue and recovery of the valuable elements. Process Safety and Environmental Protection, 128, 362–371. https://doi.org/10.1016/j.psep.2019.05.042

Zhang, D., Liu, Y., Hu, Q., Ke, X., Yuan, S., Liu, S., Ji, X., & Hu, J. (2020). Sustainable recovery of nickel, molybdenum, and vanadium from spent hydroprocessing catalysts

JIRRS
Journal International Review of Research Studies

**Received:** 13/06/2026 - **Accepted:** 07/11/2026
**Vol**: 1.11
**DOI**: 10.66104/dr86mq28
**Pages:** 1-34

by an integrated selective route. Journal of Cleaner Production, 252, 119763. https://doi.org/10.1016/j.jclepro.2019.119763

Zhang, T., Zhou, W., Li, Y., Ye, Q., Yu, X., & Chen, Z. (2022). Effect of CaO on the phase evolution of vanadium slag during crystallization and roasting–leaching processes for selective extraction of vanadium. Crystals, 12(7), 927. https://doi.org/10.3390/cryst12070927

Zhang, S.-S., Wang, Z.-Y., Hu, P., Rao, J.-T., Zong, Y.-B., & Pang, J. (2023). Influence of composition and temperature on distribution behavior of V, Ti, and Si in HIsmelt. Transactions of the Nonferrous Metals Society of China, 33(12), 3835–3846. https://doi.org/10.1016/S1003-6326(23)66374-5

Zhang, W., Ma, B., Yao, Z., Wang, K., Wang, C., Liu, Y., & Chen, Y. (2025). Multi-stage counter-current leaching and solvent extraction: A novel strategy for high-efficiency vanadium separation from high-acid slag leachate. Separation and Purification Technology, 364, 132619. https://doi.org/10.1016/j.seppur.2025.132619

Zhang, Z., Liu, T., Li, S., Chen, J., Ma, Z., Dang, J., Ying, Z., Wu, G., & Xu, S. (2026a). Efficient recovery of vanadium from vanadium–titanium slag (VTS) via calcination roasting and acid leaching: Process and mechanism. Metals, 16(5), 472. https://doi.org/10.3390/met16050472

Zhang, B., Zhang, R., Zhang, T., Dou, Z., Song, S., & Wang, Q. (2026b). Microstructure study on viscous flow and crystallization behavior of ultra-high titanium slag induced by amphoteric aluminum ions. Journal of Non-Crystalline Solids, 675, 123938. https://doi.org/10.1016/j.jnoncrysol.2025.123938

Zhang, Z., Ying, Z., Li, S., Chen, J., Liu, T., Dang, J., Ma, Z., Wu, G., & Xu, S. (2026c). Research progress on the extraction and separation technology of V and Ti in vanadium-titanium slag: A review. Journal of Environmental Management, 408, 129986. https://doi.org/10.1016/j.jenvman.2026.129986

Zhang, L., Jiang, T., Wen, J., Li, C., An, X., Li, Z., Yu, T., & Yang, G. (2026d). Selective separation and recovery of vanadium and titanium from high-acidity sulfuric leachates of $H_2$ reduction-treated vanadium-titanium slag. Journal of Environmental Chemical Engineering. https://doi.org/10.1016/j.jece.2026.125374

Zhang, L., Jiang, T., Wen, J., Hao, G., Yang, G., Yu, T., Li, C., & An, X. (2026e). Separation of iron, vanadium, and titanium from vanadium titanomagnetite concentrate by H2 reduction-magnetic separation and oxidative roasting-$H_2SO_4$ leaching. Minerals Engineering, 243, 110254. https://doi.org/10.1016/j.mineng.2026.110254

Zhao, S., Yao, Z., Ma, B., Li, X., & Wang, C. (2024a). Phase transformation and roasting kinetics of vanadium slag in an air atmosphere. Journal of Industrial and Engineering Chemistry, 133, 195–206. https://doi.org/10.1016/j.jiec.2023.11.058

Zhao, L., Zhang, X., Tan, Z., Jiang, G., Chen, Y., & Pan, D. (2024b). Recovery technology of spent hydrogenation catalysts—A review. Science of the Total Environment, 953, 176127. https://doi.org/10.1016/j.scitotenv.2024.176127

JIRRS
Journal International Review of Research Studies

**Received:** 13/06/2026 - **Accepted:** 07/11/2026
**Vol**: 1.11
**DOI**: 10.66104/dr86mq28
**Pages:** 1-34

Zhao, J., Zhang, X., Yang, F., Ai, Y., Chen, Y., & Pan, D. (2024c). Strategy and technical progress of recycling of spent vanadium–titanium-based selective catalytic reduction catalysts. ACS Omega, 9(6), 6036–6058. https://doi.org/10.1021/acsomega.3c07019

Zhao, W., Zhao, Z., Xu, Y., Cao, Z., & Zhao, T. (2025). Structural reconstruction and selective extraction of vanadium and chromium driven by calcium modification in the sodic roasting of high chromium vanadium slag. Separation and Purification Technology, 371, 133231. https://doi.org/10.1016/j.seppur.2025.133231

Zheng, F., Hu, B., Chen, G., Liu, C., Wei, J., Zhang, C., Yang, D., & He, F. (2026). Process optimization of slag composition for improved vanadium recovery and slag–iron separation in V–Ti magnetite smelting. Steel Research International, e202501151. https://doi.org/10.1002/srin.202501151

Zhou, Z., Gao, L., Rao, B., Qiao, S., & Tu, S. (2026). Research progress and prospects on vanadium extraction processes from typical vanadium-containing raw materials. Hydrometallurgy of China, 45(4), 467–475. https://doi.org/10.13355/j.cnki.sfyj.2026.04.002

Åström, E., Andersson, A., Björkman, B., & Björkvall, J. (2025). Influence of vanadium oxide on the viscosity within the $CaO–SiO_2–FeO–MgO$ system. Metallurgical and Materials Transactions B, 56, 821–832. https://doi.org/10.1007/s11663-024-03322-9